

Structural basis of the recognition of a methylated histone tail by JMJD2A

Zhongzhou Chen^{*†}, Jianye Zang^{*}, John Kappler^{**§}, Xia Hong^{*}, Frances Crawford^{**‡}, Qin Wang^{*}, Fei Lan[¶], Chengyu Jiang^{||}, Johnathan Whetstone[¶], Shaodong Dai^{**‡}, Kirk Hansen^{**}, Yang Shi[¶], and Gongyi Zhang^{*,**††}

^{*}Department of Immunology, National Jewish Medical and Research Center, Denver, CO 80206; [†]College of Biological Sciences, China Agricultural University, Beijing 100094, China; [‡]Howard Hughes Medical Institute, National Jewish Medical and Research Center, Denver, CO 80206; [¶]Department of Pathology, Harvard Medical School, Boston, MA 02115; ^{||}National Key Laboratory of Medical Molecular Biology, Peking Union Medical College, Tsinghua University and Chinese Academy of Medical Sciences, Beijing 100084, China; and ^{**}Department of Pharmacology and Cancer Center, School of Medicine, University of Colorado Health Sciences Center, Aurora, CO 80045

Contributed by John Kappler, May 14, 2007 (sent for review May 2, 2007)

The Jumonji C domain is a catalytic motif that mediates histone lysine demethylation. The Jumonji C-containing oxygenase JMJD2A specifically demethylates tri- and dimethylated lysine-9 and lysine-36 of histone 3 (H3K9/36me3/2). Here we present structures of the JMJD2A catalytic core complexed with methylated H3K36 peptide substrates in the presence of Fe(II) and *N*-oxalylglycine. We found that the interaction between JMJD2A and peptides largely involves the main chains of the enzyme and the peptide. The peptide-binding specificity is primarily determined by the primary structure of the peptide, which explains the specificity of JMJD2A for methylated H3K9 and H3K36 instead of other methylated residues such as H3K27. The specificity for a particular methyl group, however, is affected by multiple factors, such as space and the electrostatic environment in the catalytic center of the enzyme. These results provide insights into the mechanisms and specificity of histone demethylation.

demethylase | oxygenase | JmjC | epigenetic | chromatin

Covalent modification of histone proteins, which is an essential component of the regulation of gene expression in eukaryotic cells, occurs by means of a variety of enzymatic reactions (1, 2). Histone methylation has been implicated in a number of biological processes, such as heterochromatin formation, X-inactivation, genomic imprinting, and silencing of homeotic genes (3–6). Additionally, aberrant histone methylation has been linked to a number of human diseases, including cancer (7–13). Unlike other histone modifications, such as acetylation, methylation has long been considered to be a “permanent” modification. This view was based on the observation that the half-lives of histones and the histone methyl groups are similar, which suggests that histone methylation is stable and irreversible (14, 15). Recent studies, however, have shown that methylation and demethylation are widely used to posttranslationally modify histones for the regulation of gene activity. Histone demethylation is performed by two families of enzymes: the oxidases and the oxygenases (16–25). The FAD-dependent oxidase LSD1, which removes dimethyl and monomethyl groups from H3K4 and H3K9 in the presence of the androgen receptor, was the first histone demethylase to be characterized (18, 19, 23, 24). On the other hand, the Jumonji C domain-containing oxygenase family not only contains proteins that act on dimethyl and monomethyl groups, but also includes members that remove trimethyl groups from histone tails (16, 17, 20–22, 25). To understand the relationship between the structures and functions of the members of this protein family, we determined the structure of the catalytic core of the JMJD2A protein (c-JMJD2A) (16). This structure revealed several unique structural elements, including the Jumonji N domain, the Jumonji C domain, a C-terminal domain, and a zinc finger motif, which together create a potential catalytic center in the core of the protein (16). More recently, the structures of LSD1 alone and in the presence of the corepressor CoREST were determined by several groups (27–29). However,

there is no published structure of any histone demethylase in complex with a methylated peptide substrate. Therefore, a number of major points have yet to be addressed, such as the structural basis of the recognition of substrate peptides by the catalytic core and the structural features that determine the enzymatic specificity for different peptides and methyl groups. Here we describe high-resolution structures of c-JMJD2A in complex with Fe(II) and *N*-oxalylglycine (NOG) as well as a trimethylated H3K36 peptide (H3K36me3) or a monomethylated H3K36 peptide (H3K36me).

Results and Discussion

Overall Structure. Although the crystals of the complex of c-JMJD2A with a trimethylated H3K36 peptide were obtained under conditions that were different from those used to obtain the crystals of c-JMJD2A alone (16), these crystals were isomorphous and belonged to the same P21212 space group with two copies of the complex per asymmetric unit. The structure of the complex was determined by using the difference Fourier method. The $F_o - F_c$ omit map showed a region of electron density corresponding to H3K36me3 within both copies of the asymmetric unit [see supporting information (SI) Fig. 5A]. Some of the side chains of the peptide were resolved at a resolution of 2.06 Å, and conformational changes were observed in the complex structure upon binding of the peptide (SI Fig. 6). Seventeen of the peptide residues fit onto one of the c-JMJD2A molecules in an asymmetric unit, whereas 14 residues were observed on the second molecule. With the exception of the C-terminal peptide positions within the asymmetric units at which the two peptides interact with each other (SI Fig. 7), the two complexes are almost identical (Fig. 1). Overall, the curved peptide coil (yellow) lies across the surface of c-JMJD2A (Fig. 1) and contacts the long β hairpin formed by $\beta 3$ and $\beta 4$ (purple, Fig. 1), the mixed region composed of $\beta 5$ – $\alpha 5$ – $\beta 6$ (gray, Fig. 1), and the C-terminal domain between $\alpha 9$ and $\alpha 10$ (pink, Fig. 1).

Author contributions: Z.C. and G.Z. designed research; Z.C., J.Z., J.K., X.H., F.C., Q.W., F.L., and G.Z. performed research; C.J., J.W., and Y.S. contributed new reagents/analytic tools; Z.C., J.Z., J.K., S.D., K.H., and G.Z. analyzed data; and Z.C., J.Z., and G.Z. wrote the paper.

The authors declare no conflict of interest.

Freely available online through the PNAS open access option.

Abbreviation: NOG, *N*-oxalylglycine.

Data deposition: The atomic coordinates and structure factors have been deposited in the Protein Data Bank, www.pdb.org (PDB ID codes 2P5B and 2PXJ).

[§]To whom correspondence may be addressed at: Howard Hughes Medical Institute, Integrated Department of Immunology, National Jewish Medical and Research Center, 1400 Jackson Street, Denver, CO 80206. E-mail: kapplerj@njc.org.

^{††}To whom correspondence may be addressed at: Integrated Department of Immunology, National Jewish Medical and Research Center, 1400 Jackson Street, Denver, CO 80206. E-mail: zhangg@njc.org.

This article contains supporting information online at www.pnas.org/cgi/content/full/0704525104/DC1.

© 2007 by The National Academy of Sciences of the USA

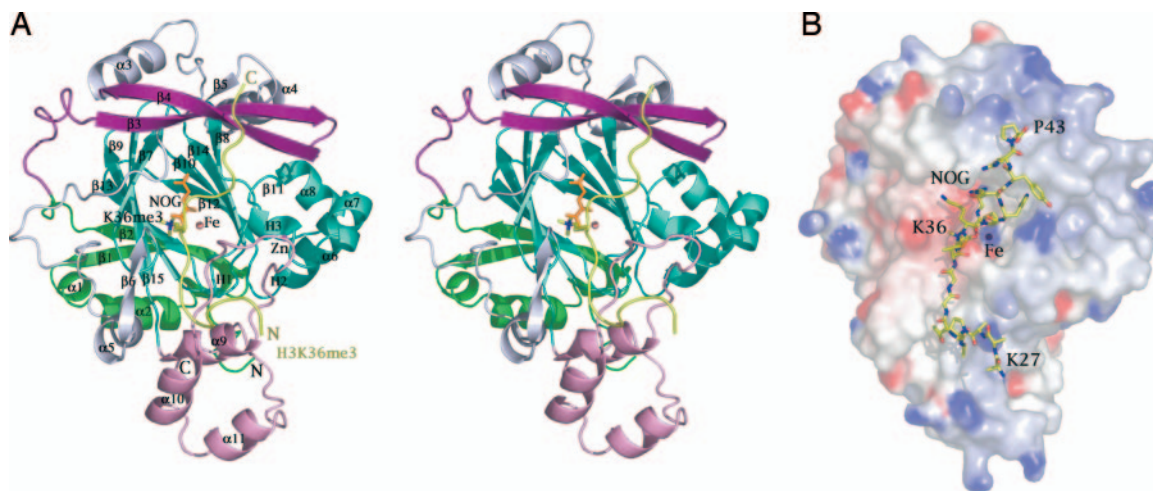


Fig. 1. The overall complex structure of c-JMJD2A with the H3K36me3 peptide in the presence of NOG (orange), Fe(II) (pink), and Zn (purple). (A) c-JMJD2A is shown as a ribbon model with the Jumonji N domain (green), the long β hairpin (purple), the mixed structural motif (gray), the Jumonji C domain (light blue), the C-terminal domain (pink), and the methylated H3K36 peptide (yellow). Seventeen of the 22 residues (residues 27–43 from histone 3) of the methylated peptide are ordered in the structure (molecule A). (B) A stick and ball model of the peptide on the surface of c-JMJD2A colored according to the electrostatic potential of the residues (red and blue represent negatively and positively charged areas, respectively). All structural figures were made by using the PyMOL program (<http://pymol.sourceforge.net>).

A comparison with all other available structures of proteins in complex with methylated peptides, including methylated peptides bound to tudor domains (30), PHD domains (31, 32), and chromodomains (33–35), did not reveal any common binding mode. This was also true when the structure was compared with complexes of DIM5 and SET7/9 bound to their cognate methylated peptides (36, 37). Based on initial mutagenesis analysis we hypothesized that the binding mode between the peptide substrate and c-JMJD2A might be similar to that of factor-inhibiting hypoxia-inducible factor (FIH) and its peptide substrate (16, 38); i.e., a sharply curved peptide coil interacts with the mixed region of c-JMJD2A (SI Fig. 8). The complex structure of c-JMJD2A and the H3K36me3 peptide, however, showed a different binding mode; although the binding of the N terminus of the peptide occurs as we previously proposed (16), the C terminus extends toward the long β hairpin (Fig. 1). The previously reported decreases in the activity of c-JMJD2A that resulted from the introduction of double mutations (16), however, can be explained by this complex structure. Mutation of Gly-133 and Gly-138 to alanine residues abolished the activity of c-JMJD2A (16); these mutations may disturb the structure of the long β hairpin or could displace Asp-135, which is involved in the interaction with the peptide (see below) (SI Fig. 9). c-JMJD2A activity was also eliminated when Gly-165 and Gly-170 were mutated to alanine residues (16). Gly-170 is involved in the formation of the methyl group-binding pocket, whereas Glu-169 interacts with the substrate peptide. BIAcore binding assays showed that these two double mutations abolished the binding of the peptide to c-JMJD2A (SI Fig. 10).

NOG is an analogue of α -ketoglutarate that mimics the initial coordination of the cofactors, substrate, and enzyme but does not initiate the hydroxylation process (38). In the current structure NOG occupies the same position and forms the same set of hydrogen bonds as α -ketoglutarate in the native structure (data not shown). Interestingly, compared with α -ketoglutarate in the native structure, NOG has a higher occupancy and lower mobility (lower thermal factor) in the crystal. One explanation for this is that the trimethylated peptide stabilizes the coordination of NOG with the other components of the complex. These findings agree with a previous study that showed that NOG inhibits the activity of c-JMJD2C and competes with α -ketoglutarate for binding (25).

Detailed Interactions. The overall surface area of c-JMJD2A covered by the bound peptide is 580 \AA^2 . Interestingly, only limited contacts were observed between c-JMJD2A and the peptide; the entire interaction between c-JMJD2A and the peptide comprises 10 hydrogen bonds and one salt bridge and involves nine residues from c-JMJD2A and eight residues from the methylated peptide (Fig. 2A). Two general characteristics of the contacts are worth noting. First, there are no apparent hydrophobic interactions involved in the binding. Second, eight of the 11 bonds are main chain–main chain interactions (Fig. 2A). In addition, the only salt bridge appears to play a crucial role in the activity of the enzyme for the substrate. Mutation of Asp-135 to Ala or Leu greatly reduced the activity of c-JMJD2A (Fig. 2B and SI Fig. 9). A similar effect was observed when Tyr-175 was mutated to Phe (Fig. 2B). Thus, minor changes in the association between the two components can lead to major effects on the efficiency or activity of the enzyme.

We used surface plasmon resonance to further analyze the binding of c-JMJD2A to H3K9me3 and H3K36me3. Biotinylated versions of the peptides were immobilized via streptavidin in the flow cells of a BIAcore biosensor chip. Various concentrations of JMJD2A were injected, and the binding data were recorded (Fig. 2C and D). Dose-dependent binding was observed for each of the peptides, whereas no binding was observed with a control peptide. For both peptides, analysis of the binding data indicated that the binding kinetics were heterogeneous and did not fit any simple kinetic model. The strongest component of the interaction had an apparent affinity of $\approx 1 \mu\text{M}$. The most obvious explanation for this heterogeneity is that the immobilized peptide could assume a number of constantly changing conformations, only some of which could bind to c-JMJD2A. Moreover, some of the amino acid side chains of the free form of c-JMJD2A may assume different conformations after peptide binding. The kinetics of the conformational changes that result from peptide binding may contribute to the heterogeneity in the observed overall kinetics of peptide binding. The fact that the enzyme readily demethylates these peptides indicates that these regions of free histones are also somewhat disordered *in vivo* but are nevertheless readily recognized by the enzyme.

Determinants of Peptide Specificity. If the interactions between c-JMJD2A and the peptide are primarily main chain–main chain

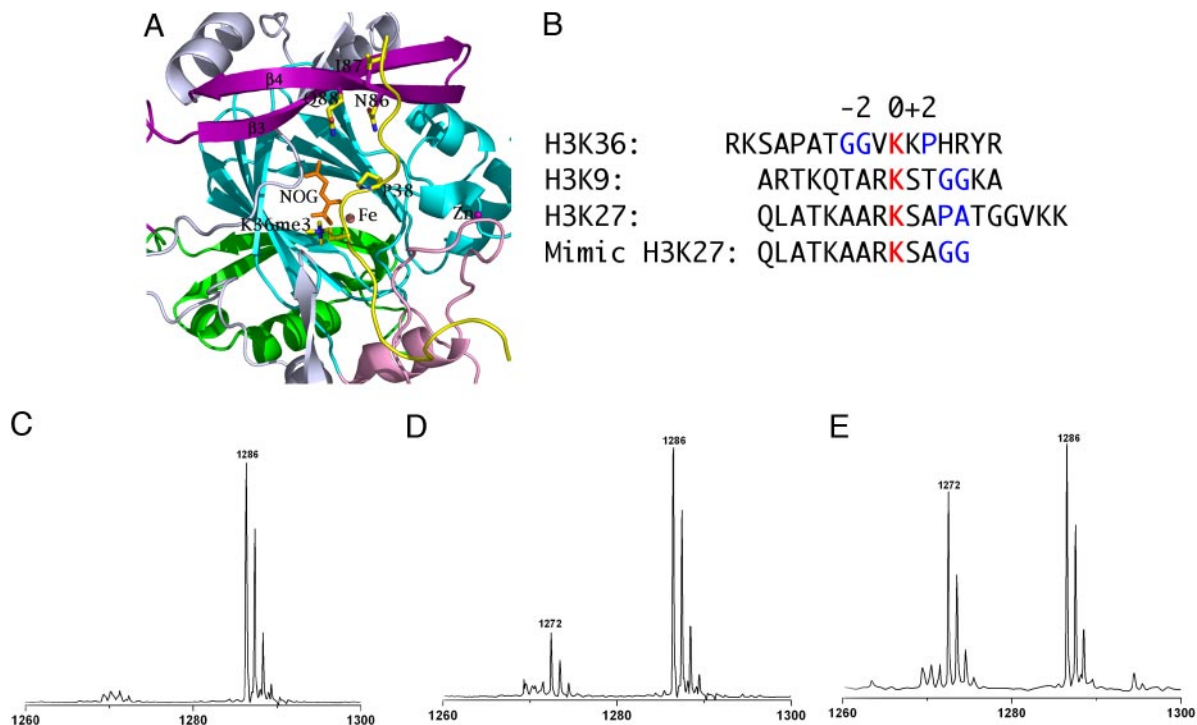


Fig. 3. Characterization of the peptide binding. (A) Pro-38 within the peptide is important for the formation of the curve in the peptide that prevents steric interference between the peptide and the long β -hairpin region of c-JMJD2A ($\beta 3$ and $\beta 4$). (B) Residues within the H3K9 and H3K36 peptides that potentially determine the specificity of peptide binding by c-JMJD2A. A proline residue at position +2 or a glycine residue at position +3 is likely to be critical for the binding. Amino acid positions are given in relation to the position of the methylated lysine residue. (C) A negative control for the demethylation assay using a mimic H3K27me2 peptide in which residues +3 and +4 from the lysine residue were mutated to Gly residues. The reaction was stopped right after the components were mixed. (D) The demethylation activity of c-JMJD2A for the mimic H3K27me2 peptide. (E) The demethylation activity of c-JMJD2D for the mimic H3K27me2 peptide.

polar environment, which includes at least two hydroxyl groups (Tyr-177 and Ser-288) and three carbonyl groups (Gly-170, Glu-190, and Asn-290), are Coulombic (the ϵ -N atom of the trimethylated Lys-36 is positively charged) (Fig. 4A). The distance between the ϵ -N atom of Lys-36 and these oxygen groups ranges from 3.52 Å to 4.67 Å, which is too far to form hydrogen bonds (Fig. 4A). Furthermore, this polar environment differs from the methyl group-binding sites described for other methylated peptide-binding proteins, which primarily employ aromatic residues to create a hydrophobic pocket that accommodates the methyl groups (31–35). This unique environment may serve two purposes. First, it may allow the methyl group involved in the reaction the freedom to assume the proper orientation (Fig. 4A and B). Second, the environment in the pocket is polar, which could be favorable for the reaction (Fig. 4B). This polar environment does appear to be required for the enzyme to function properly; mutation of Asn-290 to Ala, Leu, Ile, or Asp or mutation of Tyr-177 to Phe or Leu abolishes or reduces the activity of the enzyme (Fig. 2B).

We have previously shown that mutating Ser-288 and Thr-289 to Ala-288 and Ile-289 confers c-JMJD2A with a high level of activity for dimethyl groups (16). Comparing the model structure of this mutant variant complexed with a peptide (generated from the native structure; data not shown) and the structure of native c-JMJD2A complexed with a peptide revealed two significant features. First, these mutations generated a slightly larger pocket in the enzyme (data not shown). Second, the mutations caused the loss of the Coulombic interaction between Ser-287 and the ϵ -N atom of Lys-36. The activity for dimethyl groups was probably not a result of the additional space, because more space would actually increase the freedom of the methylated lysine side chain, thereby decreasing the chance that the methyl group will

assume the proper orientation toward the Fe(II) ion. Therefore, we believe that the loss of the Coulombic interaction is more likely to be the determining factor that results in the activity of the mutant c-JMJD2A for dimethyl groups; the altered network of Coulombic interactions fixes a methyl group in an ideal position relative to the catalytic center. Overall, we believe that a microenvironment in the methyl group-binding pocket (i.e., the network of Coulombic interactions) that pushes a methyl group toward the Fe(II) ion is the key factor that confers the enzymatic activity for specific methyl groups.

Another intriguing question is why JMJD2A and its family members do not have activity for monomethyl groups. To address this question, crystals of a complex of c-JMJD2A and H3K36me were obtained by using conditions that were similar to those used to obtain the complex of c-JMJD2A and H3K36me3. Only six residues around the K36 region were structured in the complex. The monomethyl group, however, was very well defined (SI Fig. 5B). In agreement with our hypothesis, the methyl group was turned away from the Fe(II) ion (Fig. 4C and D). The distance between the Fe(II) ion and the methyl group in the complex containing the trimethylated peptide is 4.61 Å, whereas it is 5.53 Å in the complex containing a monomethylated peptide; the larger distance may prevent the required interaction between the Fe(II) ion and the methyl group.

The Recruitment of O₂. In the catalytic center an oxygen molecule should be positioned between the Fe(II) ion and the closest methyl group. In the present complex there is an additional L-shaped area of positive electron density near this potential O₂ binding site ($F_o - F_c$ map with a 2.5- σ cutoff) (Fig. 4E). Additional water molecules, which should resemble the three nearby water molecules that are clearly defined (Fig. 4E), do not

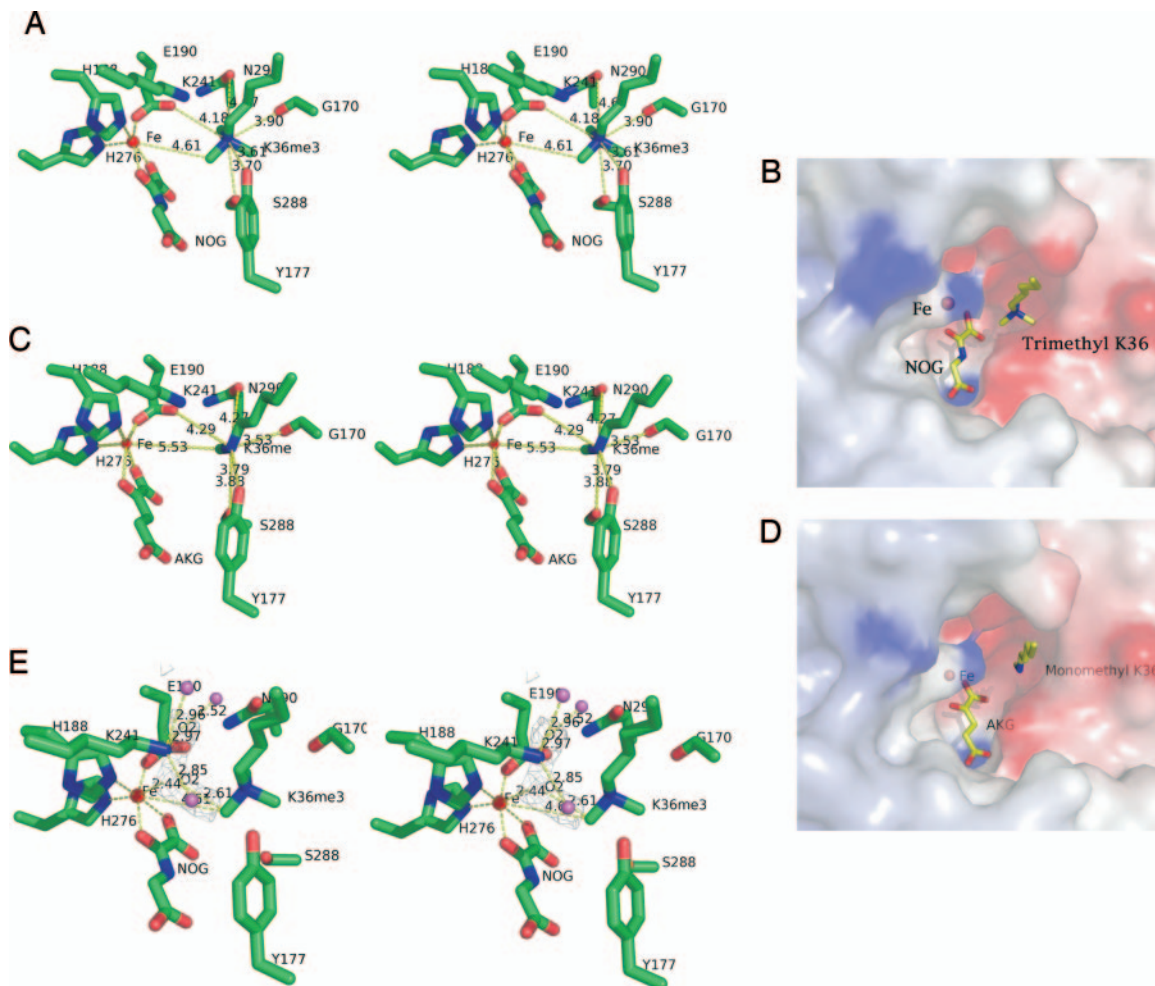


Fig. 4. The detailed methyl group-binding pocket. (A) The trimethylated Lys-36 is surrounded by a polar environment that includes hydroxyl groups from Tyr-170 and Ser-288 and carboxyl groups from Gly-170, Glu-190, and Asn-290. These moieties could form Coulombic interactions with the ϵ -N atom of Lys-36. The distance between the methyl group and the Fe(II) ion is 4.54 Å, which should allow the demethylation reaction to proceed. (B) The surface properties and space around the trimethyl group colored according to the electrostatic potential of the residues (red and blue indicate negatively and positively charged areas, respectively). (C) The monomethyl group of the peptide is positioned 5.04 Å away from the Fe(II) ion, which may explain why c-JMJD2A does not act on monomethyl groups. (D) The surface properties and space around the monomethyl group colored according to the electrostatic potential of the residues (red and blue indicate negatively and positively charged areas, respectively). (E) The potential positions of the O_2 molecule and a possible recruitment mechanism mediated by Lys-241.

fit into this site. The shape of this area indicates that the O_2 molecule can occupy two positions. In one position, the O_2 molecule interacts with the Fe(II) ion, which is participating in the reaction cycle, and the nearest methyl group (Fig. 4E). In the other position, which is not located directly between the Fe(II) ion and the methyl group, the O_2 molecule forms a hydrogen bond with the side chain of Lys-241 (Fig. 4E and SI Fig. 9), which is very well ordered in the complex structure. There is a network of hydrogen bonds between the three water molecules, the ϵ -N atom of Lys-241, and the O_2 molecule when it is not positioned between the Fe(II) ion and the methyl group. This structure suggests that the O_2 molecule is recruited by Lys-241 and is then delivered to the position between the Fe(II) ion and the methyl group to participate in the reaction. To test whether the side chain of Lys-241 is involved in the enzymatic reaction, Lys-241 was mutated to Ala or Leu. In support of our model, each of these mutations completely abolished the activity of c-JMJD2A (Fig. 2B).

Structural determination and functional characterization of the complexes of c-JMJD2A and the H3K36me3 or H3K36me peptide revealed a number of novel features regarding substrate

recognition, specificity determination, and the reaction mechanism. This structure, however, also raises a number of new questions. For example, because substituting all of the residues on the surface of JMJD2D involved in peptide recognition with the corresponding residues from JMJD2A does not confer JMJD2D with activities for dimethylated and trimethylated H3K36 peptides, the atomic basis of the differential activities of these enzymes for dimethylated or trimethylated H3K36 remains unclear. Furthermore, although JHDM1 shows activity for the same H3K36me2 substrate, structure-based sequence alignment combined with secondary structure prediction suggests that this protein is dramatically different from the JMJD2 family in all four major areas that create the peptide-binding site in c-JMJD2A with the exception of the cupin fold (data not shown). Structural analyses of a variety of homologues and different family members with and without substrate peptides combined with functional characterization of these proteins *in vivo* should provide answers to these questions.

Materials and Methods

Protein Expression, Purification, and Crystallization. c-JMJD2A and the mutant variants were expressed and purified as described

(16, 21). The complexes of c-JMJD2A, the cofactors, and the trimethylated or monomethylated peptides (RKSAPATG-GVKKPHRYRPGTVK) were crystallized by vapor diffusion at 4°C against a solution containing 200 mM MgCl₂, 100 mM Tris (pH 8.5), and 13–15% PEG5K. For data collection, crystals were gradually transferred to a cryo buffer (reservoir buffer supplemented with 20% glycerol) and flash-cooled in liquid N₂. All data used for the structure solution and refinements were collected on beamline 8.2.2 at the Advanced Light Source (Berkeley, CA). Data were integrated and scaled with the HKL2000 suite of programs (39).

Structure Determination and Refinement. Structures of the complexes were solved by using the difference Fourier method and the model of c-JMJD2A (16). After one round of energy minimization with the c-JMJD2A model in the Crystallography and NMR System (40), $2F_o - F_c$ and $F_o - F_c$ maps were calculated. The initial peptide models were manually built by using the program O (26). The models were refined against the data collected from several crystals to a resolution of 2.06 Å for the trimethyl complex and 2.0 Å for the monomethyl complex using the Crystallography and NMR System (40). The two-fold noncrystallographic symmetry restraints were applied during refinement. The final models contain amino acid residues 2–348 of molecule A and residues 2–346 of molecule B. For the trimethyl complex 17 peptide residues were ordered on molecule A whereas 14 peptide residues were ordered on molecule B. Only six residues are structured on both molecules of the monomethyl complex. There are two NOG molecules, two Fe(II) ions, and two Zn ions in the final refined models. Structure refinement statistics are shown in SI Table 1. The coordinates of the complex structures have been deposited in the Protein Data Bank with ID codes 2P5B and 2PXJ.

Demethylation Activity Assays. Details of the demethylation reactions and detection by MALDI-TOF mass spectrometry have been described previously (16, 21).

Surface Plasmon Resonance Binding Assays. Surface plasmon resonance experiments were performed by using a BIAcore 2000 instrument with a streptavidin-containing BIA sensor SA chip. C-terminally biotinylated versions of the H3K9 (ART-KQTARKSTGGKAPRKQLAK) and H3K36 (the same sequence used for cocrystallization except for the biotinylation) peptides were obtained from AnaSpec (San Jose, CA). A biotinylated peptide from mouse heat shock protein 70 (biotin-GGGGDRMVNHFIAEFKRRK) was used as a negative control. The peptides were immobilized by streptavidin capture in three flow cells of the BIA sensor chip. Using a running buffer of 150 mM NaCl and 10 mM Hepes (pH 7.2), various concentrations of JMJD2A were injected through the three peptide-containing flow cells and through a fourth flow cell that did not contain the peptide at a rate of 10 μl/min for 1 min. The sensorgram obtained for the flow cell containing no peptide was subtracted from those obtained with each peptide to correct for any nonspecific binding and the bulk signal from the protein in solution. The data were analyzed with BIAevaluation 4.1 software.

We thank Dr. Xin Bi (University of Rochester, Rochester, NY) and Dr. Denis Volker (National Jewish Medical and Research Center) for genomic DNA from budding and fission yeast; Dr. James Kappler for editing; the Howard Hughes Medical Institute, the Zuckerman/Canyon Ranch, and Alan Lapporte for support of our x-ray and computing facility; the Proteomics Core Center at the University of Colorado Cancer Center for mass spectrometry access; and Dr. Philippa C. Marrack, Dr. James D. Crapo, and other researchers at the National Jewish Medical and Research Center for their kind support. All data sets were collected at the Howard Hughes Medical Institute beamline 8.2.2 at the Advanced Light Source. Z.C. is supported by a Viola Vestal Coulter Scholarship. Y.S. is supported by National Institutes of Health Grants GM058012 and GM071004. G.Z. is supported by National Institutes of Health Grants AI22295 (to Philippa C. Marrack) and GM80719 as well as National Natural Science Foundation of China Grant 30528002.

- Jenuwein T, Allis CD (2001) *Science* 293:1074–1080.
- Strahl BD, Allis CD (2000) *Nature* 403:41–45.
- Kouzarides T (2002) *Curr Opin Genet Dev* 12:198–209.
- Lachner M, Jenuwein T (2002) *Curr Opin Cell Biol* 14:286–298.
- Margueron R, Trojer P, Reinberg D (2005) *Curr Opin Genet Dev* 15:163–176.
- Martin C, Zhang Y (2005) *Nat Rev Mol Cell Biol* 6:838–849.
- Fraga MF, Esteller M (2005) *Cell Cycle* 4:1377–1381.
- Hake SB, Xiao A, Allis CD (2004) *Br J Cancer* 90:761–769.
- Schneider R, Bannister AJ, Kouzarides T (2002) *Trends Biochem Sci* 27:396–402.
- Varambally S, Dhanasekaran SM, Zhou M, Barrette TR, Kumar-Sinha C, Sanda MG, Ghosh D, Pienta KJ, Sewalt RG, Otte AP, et al. (2002) *Nature* 419:624–629.
- Hess JL (2004) *Trends Mol Med* 10:500–507.
- Hess JL (2004) *Crit Rev Eukaryotic Gene Expression* 14:235–254.
- Okada Y, Feng Q, Lin Y, Jiang Q, Li Y, Coffield VM, Su L, Xu G, Zhang Y (2005) *Cell* 121:167–178.
- Byvoet P, Shepherd GR, Hardin JM, Noland BJ (1972) *Arch Biochem Biophys* 148:558–567.
- Thomas G, Lange HW, Hempel K (1972) *Hoppe-Seyler's Z Physiol Chem* 353:1423–1428.
- Chen Z, Zang J, Whetstine J, Hong X, Davrazou F, Kutateladze TG, Simpson M, Mao Q, Pan CH, Dai S, et al. (2006) *Cell* 125:691–702.
- Klose RJ, Yamane K, Bae Y, Zhang D, Erdjument-Bromage H, Tempst P, Wong J, Zhang Y (2006) *Nature* 442:312–316.
- Lee MG, Wynder C, Cooch N, Shiekhhattar R (2005) *Nature* 437:432–435.
- Shi Y, Lan F, Matson C, Mulligan P, Whetstine JR, Cole PA, Casero RA, Shi Y (2004) *Cell* 119:941–953.
- Yamane K, Toumazou C, Tsukada YI, Erdjument-Bromage H, Tempst P, Wong J, Zhang Y (2006) *Cell* 125:483–495.
- Whetstine JR, Nottke A, Lan F, Huarte M, Smolikov S, Chen Z, Spooner E, Li E, Zhang G, Colaiacovo M, Shi Y (2006) *Cell* 125:167–181.
- Tsukada Y, Fang J, Erdjument-Bromage H, Warren ME, Borchers CH, Tempst P, Zhang Y (2006) *Nature* 439:811–816.
- Shi YJ, Matson C, Lan F, Iwase S, Baba T, Shi Y (2005) *Mol Cell* 19:857–864.
- Metzger E, Wissmann M, Yin N, Muller JM, Schneider R, Peters AH, Gunther T, Buettner R, Schule R (2005) *Nature* 437:436–439.
- Cloos PA, Christensen J, Agger K, Maiolica A, Rappsilber J, Antal T, Hansen KH, Helin K (2006) *Nature* 442:307–311.
- Jones TA, Zou JY, Cowan SW, Kjeldgaard M (1991) *Acta Crystallogr A* 47:110–119.
- Da G, Lenkart J, Zhao K, Shiekhhattar R, Cairns BR, Marmorstein R (2006) *Proc Natl Acad Sci USA* 103:2057–2062.
- Stavropoulos P, Blobel G, Hoelz A (2006) *Nat Struct Mol Biol* 13:626–632.
- Yang M, Goeckel CB, Luo X, Borek D, Tomchick DR, Machius M, Otwinowski Z, Yu H (2006) *Mol Cell* 23:377–387.
- Huang Y, Fang J, Bedford MT, Zhang Y, Xu RM (2006) *Science* 312:748–751.
- Pena PV, Davrazou F, Shi X, Walter KL, Verkhusha VV, Gozani O, Zhao R, Kutateladze TG (2006) *Nature* 442:100–103.
- Li H, Ilin S, Wang W, Duncan EM, Wysocka J, Allis CD, Patel DJ (2006) *Nature* 442:91–95.
- Nielsen PR, Nietlispach D, Mott HR, Callaghan J, Bannister A, Kouzarides T, Murzin AG, Murzina NV, Laue ED (2002) *Nature* 416:103–107.
- Flanagan JF, Mi LZ, Chruszcz M, Cymborowski M, Clines KL, Kim Y, Minor W, Rastinejad F, Khorasanizadeh S (2005) *Nature* 438:1181–1185.
- Jacobs SA, Khorasanizadeh S (2002) *Science* 295:2080–2083.
- Zhang X, Yang Z, Khan SI, Horton JR, Tamaru H, Selker EU, Cheng X (2003) *Mol Cell* 12:177–185.
- Xiao B, Jing C, Wilson JR, Walker PA, Vasisth N, Kelly G, Howell S, Taylor IA, Blackburn GM, Gamblin SJ (2003) *Nature* 421:652–656.
- Elkins JM, Hewitson KS, McNeill LA, Seibel JF, Schlemminger I, Pugh CW, Ratcliffe PJ, Schofield CJ (2003) *J Biol Chem* 278:1802–1806.
- Otwinowski Z, Borek D, Majewski W, Minor W (2003) *Acta Crystallogr A* 59:228–234.
- Brunger AT, Adams PD, Clore GM, DeLano WL, Gros P, Grosse-Kunstleve RW, Jiang JS, Kuszewski J, Nilges M, Pannu NS, et al. (1998) *Acta Crystallogr D* 54:905–921.